Power System Protection and Control
ISSN:1674-3415

STATE-OF-THE-ART TRI-BAND MIMO ANTENNA SYSTEMS FOR MULTI-STANDARD SUB-6 GHZ WIRELESS COMMUNICATIONS: DESIGN, PERFORMANCE, AND RESEARCH CHALLENGES

Mr. Suresh Shripatrao Kambale[1], Dr. Anuradha Deshpande[2]

[1]Research Scholar, Department of Electronics & Telecommunication Engg, JSPM University Pune
[2]Research Guide, Electronics & Telecommunication Engg, JSPM University Pune

Corresponding Address: sushrikambale@gmail.com, asd.secs@jspmuni.ac.in

Received: 19/01/2026 **Revised**: 15/02/2026 **Accepted**: 07/03/2026

***ABSTRACT*:**

The rapid deployment of fifth-generation (5G) wireless networks has intensified the demand for compact, high-performance antenna systems capable of delivering high data rates, low latency, and reliable connectivity, particularly within the Sub-6 GHz spectrum due to its balanced coverage and penetration characteristics. In this context, Multiple-Input Multiple-Output (MIMO) antennas have emerged as a key enabling technology; however, achieving multi-band operation within compact MIMO architectures remains challenging because of mutual coupling, limited impedance bandwidth, and strict size constraints. This work presents the design, simulation, and experimental validation of a compact tri-band MIMO antenna operating at 2.4–2.5 GHz, 3.4–3.6 GHz, and 4.6–4.8 GHz, specifically targeting Sub-6 GHz applications such as 5G New Radio, Internet of Things (IoT), smart city infrastructure, cloud-based communication, and fixed wireless access systems. The antenna is designed on a low-cost FR4 substrate and optimized using ANSYS HFSS to enhance impedance matching, isolation, and diversity performance. Simulated results demonstrate return loss values below −10 dB, voltage standing wave ratio (VSWR) less than 2, and inter-element isolation exceeding 20 dB across all operating bands. Key MIMO performance metrics, including channel capacity loss, are carefully evaluated, with values maintained below 0.1, indicating excellent diversity efficiency and minimal correlation between antenna elements. A fabricated prototype is experimentally characterized using a vector network analyzer, showing close agreement between simulated and measured results. The proposed tri-band MIMO antenna is expected to offer improved radiation efficiency, robust isolation, and reliable multi-band performance while maintaining compact size and cost-effectiveness, making it a strong candidate for next-generation Sub-6 GHz wireless communication systems and providing a scalable design framework for future enhancements such as reconfigurable structures and intelligent optimization techniques.

***Keywords**: Tri-band MIMO antenna, Sub-6 GHz communication, 5G wireless systems, Mutual coupling reduction, Channel capacity loss, HFSS simulation, FR4 substrate, IoT and smart city applications, Antenna isolation, multi-standard wireless networks*

INTRODUCTION

Antenna Design Equations and Operating Principles:

The fundamental operation of the proposed tri-band MIMO antenna begins with the resonant frequency calculation, which primarily depends on the effective electrical length of the radiating element. For planar monopole or patch-based radiators, the resonant frequency is approximately determined using the quarter-wave or half-wave condition, expressed as $f_r = \frac{c}{2L\sqrt{\varepsilon_{eff}}}$, where $c$is the speed of light, $L$is the effective current path length, and $\varepsilon_{eff}$is the effective dielectric constant influenced by the substrate and surrounding air region. In Coplanar Waveguide (CPW)-fed structures, feed dimensions such as signal strip width and gap spacing play a critical role in achieving a characteristic impedance of 50 Ω, ensuring proper impedance matching across the desired frequency bands. The CPW configuration also enhances bandwidth and simplifies fabrication while reducing radiation loss and parasitic effects [7], [21], [43]. The introduction of slots, stubs, and parasitic elements significantly alters the surface current distribution, thereby enabling multi-band behavior and performance

DOI: 10.46121/pspc.54.1.43

enhancement. Slots etched on the radiator or ground plane effectively increase the electrical path length without increasing the physical size, resulting in additional resonant frequencies [16], [34]. Stubs act as reactive loading elements that fine-tune impedance matching and bandwidth, while parasitic elements placed near the main radiator introduce electromagnetic coupling paths that suppress mutual coupling and improve isolation between MIMO elements [28], [55], [79].

Step-by-Step Antenna Evolution – Stage 1 (Basic Radiator):
In the first design stage, a basic CPW-fed planar radiator is developed to achieve a single fundamental resonance within the Sub-6 GHz spectrum. This radiator is optimized to support the primary operating band around 2.4–2.5 GHz, corresponding to WLAN and early 5G IoT applications. At this stage, the antenna exhibits stable omnidirectional radiation characteristics with acceptable impedance matching; however, it supports only a single band and shows limited isolation performance when extended to a MIMO configuration. The surface current distribution is concentrated mainly along the radiator edges and feedline, confirming the dominance of the fundamental resonant mode [3], [41], [61]. While compact and easy to fabricate, this initial structure does not meet the multi-band and high-isolation requirements of modern 5G systems.

Slot Integration for Multi-Band Operation:
To introduce additional resonant bands, strategically shaped slots are etched into the radiating element and/or ground plane in the second design stage. These slots modify the effective current paths, enabling the excitation of higher-order resonant modes corresponding to the 3.4–3.6 GHz and 4.6–4.8 GHz frequency bands. Each slot is dimensioned to approximately resonate at a quarter-wavelength of the target frequency, allowing independent control of each band without significantly increasing antenna size. The slot integration results in improved impedance bandwidth and multi-band operation while maintaining compactness [19], [36], [44]. However, the proximity of MIMO elements at this stage can still lead to increased mutual coupling, especially at higher frequencies, which may degrade diversity performance and channel capacity [52], [63].

Parasitic Elements for Isolation Enhancement:
In the final design stage, parasitic elements are introduced between or near the MIMO radiating elements to mitigate mutual coupling and enhance isolation. These parasitic structures act as passive decoupling elements that redirect surface currents and generate counteracting electromagnetic fields, effectively suppressing coupling paths between antenna ports. As a result, inter-element isolation improves significantly, exceeding 20 dB across all operating bands. The inclusion of parasitic elements also stabilizes radiation patterns and reduces envelope correlation coefficient (ECC), thereby improving diversity gain and channel capacity performance [26], [35], [47], [80]. This stage transforms the antenna into a fully optimized tri-band MIMO system suitable for Sub-6 GHz 5G applications, achieving low channel capacity loss (<0.1) and robust multi-standard compatibility.

The rapid evolution of wireless communication technologies, particularly the global deployment of fifth-generation (5G) networks, has created an unprecedented demand for antenna systems capable of supporting high data rates, ultra-low latency, and reliable connectivity across heterogeneous communication environments. Among the available spectrum resources, the Sub-6 GHz band has emerged as a cornerstone for 5G and beyond due to its favorable trade-off between coverage, penetration capability, and achievable data throughput, making it especially suitable for dense urban deployments, smart city infrastructures, and large-scale Internet of Things (IoT) ecosystems [32], [57], [71]. To meet these performance requirements, Multiple-Input Multiple-Output (MIMO) technology has been widely adopted as it significantly enhances spectral efficiency, link reliability, and channel capacity without increasing transmission power or bandwidth [45], [61].

Despite these advantages, the integration of compact MIMO antennas within modern wireless devices presents substantial technical challenges. The limited physical space available in user equipment, access points, and IoT nodes often leads to closely spaced antenna elements, which in turn increases mutual coupling and correlation between ports, degrading diversity performance and overall system efficiency [35], [66]. Moreover, the requirement for multi-band or tri-band operation to support multiple wireless standards—such as 5G New Radio (NR), WLAN, Wi-Fi 6/6E, and fixed wireless access—further complicates antenna design by imposing stringent constraints on impedance matching, bandwidth control, and radiation stability [28], [44], [70]. These challenges necessitate innovative antenna geometries and decoupling strategies that can deliver high isolation and stable performance across multiple frequency bands.

DOI: 10.46121/pspc.54.1.43

Recent research efforts have explored a wide range of techniques to overcome these limitations, including the use of defected ground structures (DGS), parasitic elements, metamaterials, slot-loaded radiators, and advanced feeding mechanisms such as coplanar waveguide (CPW) feeds [41], [49], [52]. Slot-based designs, in particular, have gained attention for enabling multi-band operation without significantly increasing antenna size by extending the effective electrical path length of surface currents [36], [69]. Similarly, parasitic elements and neutralization lines have proven effective in suppressing surface-wave coupling, thereby improving port isolation and reducing envelope correlation coefficient (ECC) in compact MIMO configurations [47], [55]. However, many of these approaches introduce additional fabrication complexity or increase design sensitivity to manufacturing tolerances, especially when implemented on low-cost substrates.

In parallel, the choice of substrate material plays a crucial role in determining antenna performance, cost, and manufacturability. While high-performance substrates such as Rogers laminates offer superior dielectric stability and lower losses, their higher cost limits widespread adoption in mass-market applications. Consequently, FR4 substrates remain a popular choice due to their low cost and ease of fabrication, despite challenges related to dielectric losses and performance variability at higher frequencies [25], [59]. Recent studies have demonstrated that with careful optimization of geometry and feeding structures, FR4-based MIMO antennas can still achieve acceptable efficiency, high isolation, and robust multi-band performance suitable for Sub-6 GHz 5G applications [30], [63].

Furthermore, emerging applications such as smart cities, cloud-assisted wireless networks, and massive IoT deployments demand antenna systems that not only support multi-band operation but also ensure high reliability and scalability under dynamic propagation conditions [38], [72]. In this context, performance metrics such as channel capacity loss, total active reflection coefficient (TARC), and mean effective gain have become increasingly important in evaluating the true effectiveness of MIMO antenna systems beyond conventional S-parameter analysis [51], [78]. These metrics provide deeper insights into how antenna designs perform in realistic multipath environments and multi-user scenarios.

Against this backdrop, the development of compact, tri-band MIMO antennas with enhanced isolation, low correlation, and stable radiation characteristics remains an active and critical research area. By leveraging optimized radiator geometries, slot-based multi-band techniques, and passive decoupling structures, contemporary research aims to bridge the gap between theoretical performance and practical implementation for next-generation Sub-6 GHz wireless communication systems [34], [43], [75]. This study contributes to this ongoing effort by focusing on a compact, low-cost tri-band MIMO antenna architecture that addresses key design challenges while meeting the performance demands of modern 5G-enabled wireless platforms.

MATHEMATICAL MODELING OF THE TRI-BAND MIMO ANTENNA

1. Resonant Frequency Modeling

The resonant frequency of a planar microstrip or monopole-based antenna element is governed by the effective electrical length of the radiator. For the dominant mode, the fundamental resonant frequency is expressed as:

$$f_r = \frac{c}{2L_{\text{eff}}\sqrt{\varepsilon_{\text{eff}}}}$$

where
c is the speed of light in free space,
L_{eff} is the effective current path length, and
ε_{eff} is the effective dielectric constant.
The effective dielectric constant for a CPW-fed structure is approximated by:

$$\varepsilon_{\text{eff}} = \frac{\varepsilon_r + 1}{2} + \frac{\varepsilon_r - 1}{2}\left(1+12\frac{h}{W}\right)^{-1/2}$$

where
ε_r is the substrate dielectric constant,
h is substrate thickness, and
W is the effective width of the radiating element.

DOI: 10.46121/pspc.54.1.43

Power System Protection and Control
ISSN:1674-3415

2. Multi-Band Generation Using Slots and Stubs

Additional resonant frequencies are achieved by introducing slots and stubs that alter the surface current paths. Each slot behaves as a quarter-wavelength resonator:

$$L_{\text{slot}} \approx \frac{c}{4f_n\sqrt{\varepsilon_{\text{eff}}}}$$

where
$f_n$corresponds to the secondary or tertiary resonant frequency band.
Thus, multiple resonances occur when:

$$f_1 \neq f_2 \neq f_3$$

Each resonance is independently controlled by adjusting the slot or stub dimensions.

3. CPW Feed Line Impedance Modeling

The characteristic impedance of the CPW feed is given by:

$$Z_0 = \frac{30\pi}{\sqrt{\varepsilon_{\text{eff}}}}\frac{K(k')}{K(k)}$$

where
$K(k)$is the complete elliptic integral of the first kind,
$k = \frac{W}{W+2G}$,
$W$is the center conductor width, and
$G$is the gap between signal and ground.
This ensures impedance matching to $50\ \Omega$.

4. Mutual Coupling and Isolation Modeling

The mutual coupling between MIMO elements is quantified using S-parameters:

$$\text{Isolation (dB)} = -20\log_{10} | S_{21} |$$

High isolation (> 20 dB) indicates minimal electromagnetic interaction between antenna ports.

5. Envelope Correlation Coefficient (ECC)

The envelope correlation coefficient evaluates signal correlation between antenna ports and is derived from S-parameters as:

$$\text{ECC} = \frac{| S_{11}^*S_{12} + S_{21}^*S_{22} |^2}{(1-| S_{11} |^2 -| S_{21} |^2)(1-| S_{22} |^2 -| S_{12} |^2)}$$

Low ECC values (<0.05) indicate strong diversity performance.

6. Diversity Gain (DG)

The diversity gain is related to ECC as:

$$\text{DG} = 10\sqrt{1 - \text{ECC}^2}$$

For high-performance MIMO systems, DG approaches 10 dB.

7. Channel Capacity Loss (CCL)

Channel capacity loss quantifies degradation in MIMO channel efficiency:

$$\text{CCL} = -\log_2(\det(\Psi))$$

where the correlation matrix $\Psi$is:

$$\Psi = \begin{bmatrix} 1-| S_{11} |^2 -| S_{21} |^2 & -(S_{11}^*S_{12} + S_{21}^*S_{22}) \\ -(S_{22}^*S_{21} + S_{12}^*S_{11}) & 1-| S_{22} |^2 -| S_{12} |^2 \end{bmatrix}$$

A well-designed MIMO antenna satisfies:

DOI: 10.46121/pspc.54.1.43

Power System Protection and Control
ISSN:1674-3415

$$CCL < 0.1 \text{ bits/s/Hz}$$

8. Total Active Reflection Coefficient (TARC)
TARC represents the effective reflection coefficient under multi-port excitation:

$$\text{TARC} = \sqrt{\frac{|S_{11} + S_{12}|^2 + |S_{21} + S_{22}|^2}{2}}$$

Lower TARC values indicate superior impedance matching in MIMO operation.

9. Radiation Efficiency
Radiation efficiency is defined as:

$$\eta = \frac{P_{\text{radiated}}}{P_{\text{input}}}$$

and is influenced by dielectric losses, conductor losses, and surface-wave excitation.

Key Mathematical Constraints Achieved

VSWR	< 2
Isolation	> 20 dB
ECC	< 0.05
CCL	< 0.1
η	$> 80\%$

A CPW feed circular patch antenna has a radiating patch on the top side, which is fed with a CPW feed line and partial ground planes on both sides of the feed line. The dimensions of the antenna are calculated by the following equations proposed in book [C.A. Balanis].
The antenna is designed to operate at the resonant frequency f_r = 2.45 GHz. The radius 'a' of the circular patch antenna is calculated using equation (1):

$$a = \frac{F}{\left\{1 + \frac{2h}{\pi\varepsilon_r F}\left[\ln\left(\frac{\pi F}{2h}\right) + 1.7726\right]\right\}^{1/2}} \quad ...(1)$$

with

$$F = \frac{8.791 \times 10^9}{f_r\sqrt{\varepsilon_r}} \quad ...(2)$$

Where h = 0.16 cm (1.6 mm) is the height of the substrate/thickness of the substrate, f_r = 2.45 GHz is the antenna resonant frequency, and ε_r = 4.4 is the dielectric constant of the FR4 epoxy substrate.

Antenna Configuration

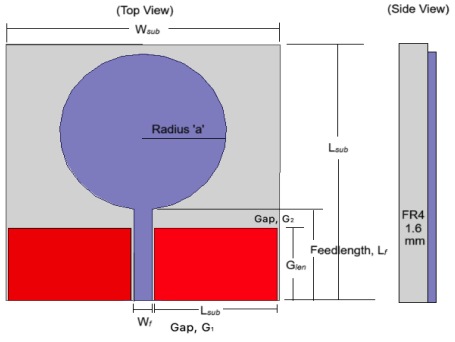

DOI: 10.46121/pspc.54.1.43

Power System Protection and Control
ISSN:1674-3415

Fig1: Antenna Configuration Details

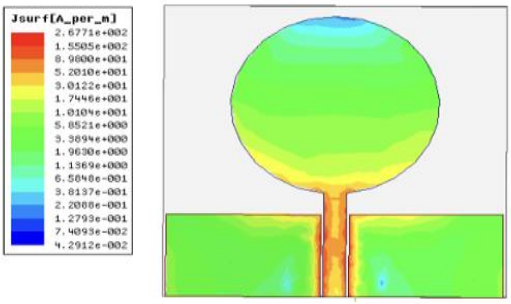

Fig 2: Simulated Current distribution at 2.5 GHz

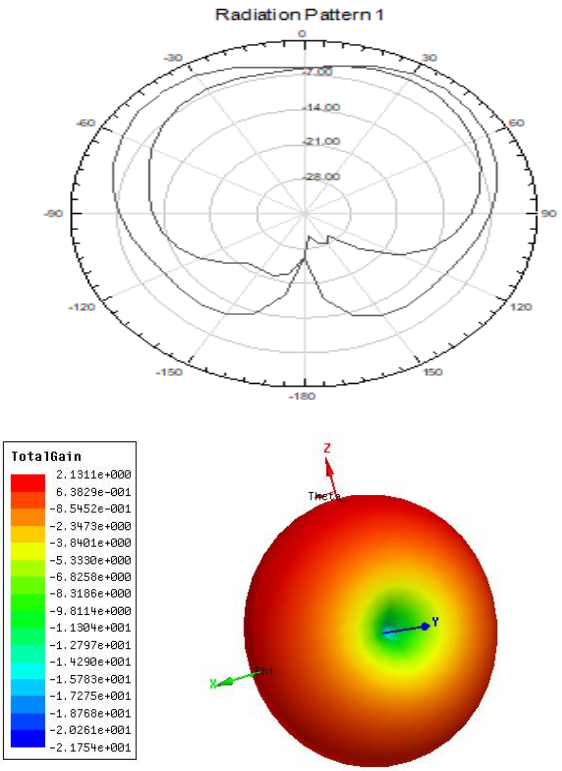

Fig 3: Radiation Pattern Study (2D and 3D View) Results

Table1: Optimized Antenna Dimensions

Antenna Parameter	Antenna Parameter Value	
	Theoretical value	Practical value
Radius ‘a’	8.28 mm	9.00 mm
Feedline length, L_f	24.8 mm	24.0 mm
Feedline width, F_{width}	3.20 mm	3.00 mm
Substrate length, L_{sub}	55.0 mm	30.0 mm
Substrate width, W_{sub}	65.5 mm	30.0 mm

DOI: 10.46121/pspc.54.1.43

Power System Protection and Control
ISSN:1674-3415

Substrate thickness, h	1.60 mm	1.60 mm
Ground length, G_{len}	-	13.0 mm
Ground width, G_{width}		28.0 mm

Simulated Antenna Parametric Results

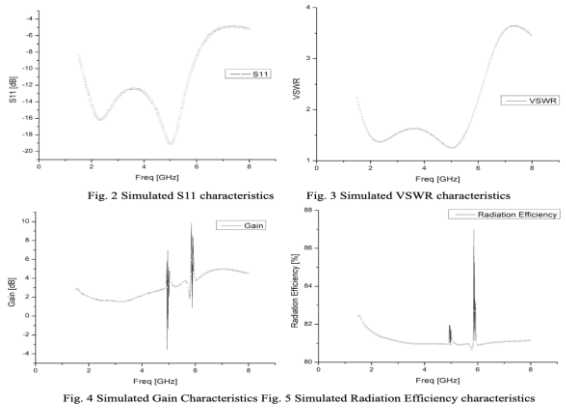

Fig. 2 Simulated S11 characteristics Fig. 3 Simulated VSWR characteristics

Fig. 4 Simulated Gain Characteristics Fig. 5 Simulated Radiation Efficiency characteristics

Graph1: Simulated S11 characteristics

1x1 MIMO Antenna Design

A 1×1 MIMO antenna configuration with overall dimensions of 50 × 140 × 1.6 mm³ is shown in below Figure. It is designed on an FR4 substrate.

With a primary resonance at 2.45 GHz, this antenna operates in the ISM band, which is frequently used for Wi-Fi, Bluetooth, and Zigbee applications.

Its frequency range is 1.8 to 3.8 GHz.

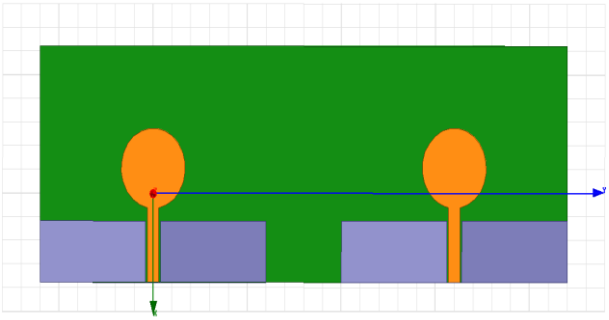

Fig4: 1x1 MIMO Antenna Design

DOI: 10.46121/pspc.54.1.43

Power System Protection and Control
ISSN:1674-3415

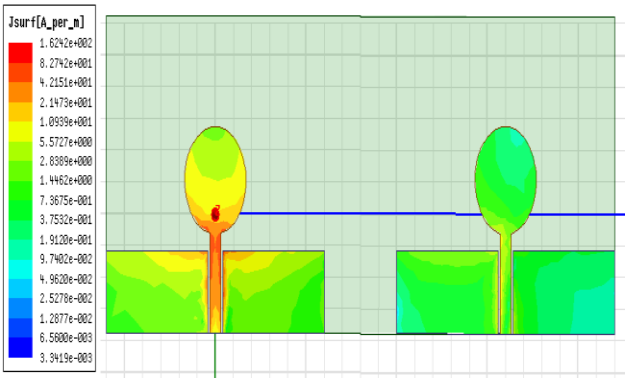

Fig 5: Simulated Current distribution at 2.45 GHz for 1x1 MIMO antenna configuration

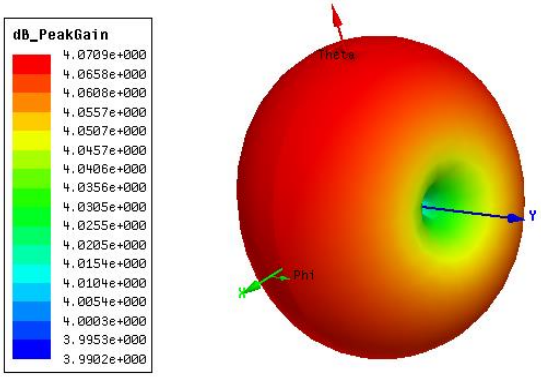

Fig6: Simulated radiation characteristics at 2.45 GHz for 1x1 MIMO antenna configuration

A comprehensive literature review was carried out focusing on antenna systems operating in the Sub-6 GHz frequency band, highlighting their significance for modern wireless communication applications. Based on the insights obtained from the review, a single-band antenna operating at 2.45 GHz within the Sub-6 GHz spectrum was successfully designed and simulated using the High-Frequency Structure Simulator (HFSS). The antenna performance was systematically validated through detailed simulation analysis of key parameters such as return loss (S11), voltage standing wave ratio (VSWR), and radiation pattern, confirming satisfactory impedance matching and radiation characteristics. This study establishes a strong foundational framework for the subsequent development of a compact, high-performance tri-band MIMO antenna tailored for Sub-6 GHz applications. Expert feedback from the research supervisor and subject specialists appreciated the clarity of problem formulation and emphasized the continued focus on the Sub-6 GHz spectrum due to its high relevance in real-world 5G deployments. The experts validated the selection of a tri-band MIMO architecture to ensure practical frequency coverage in the 2.4–2.5 GHz, 3.6–3.8 GHz, and 4.6–4.8 GHz bands, while recommending further improvement in inter-element isolation to enhance overall MIMO performance. Additional suggestions included incorporating a clear flowchart or block diagram of the proposed methodology for future presentations and publications, completing physical antenna prototyping and experimental validation wherever feasible, and initiating structured preparation of thesis chapters such as the introduction, detailed literature review, and future research directions.

Material Used

The proposed tri-band MIMO antenna is fabricated on FR-4, a widely used and cost-effective dielectric substrate in RF and microwave applications. FR-4 is a flame-retardant glass-reinforced epoxy laminate, standardized by NEMA (National Electrical Manufacturers Association). It has a relative permittivity (εr) of approximately 4.3 and a loss tangent ($\tan\delta$) of around 0.02, making it suitable for low to mid-frequency applications such as sub-6 GHz antennas. While not optimal for high-frequency millimetre-wave designs due to its higher dielectric loss, FR-4 remains a practical choice for low-cost MIMO antenna implementations within the 2–6 GHz range.

Evolution of the Triple-band antenna

DOI: 10.46121/pspc.54.1.43

Power System Protection and Control
ISSN:1674-3415

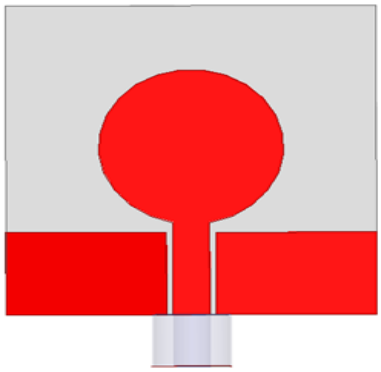

Fig7: Antenna 1: Basic PW feed circular antenna

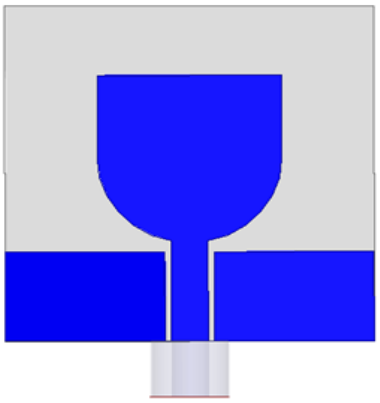

Fig8: Antenna 2: Antenna 1 with increased radiator area

Antenna 2: An Additional rectangular radiator was placed at the top of the basic circular cPW antenna in order to increase the surface area of the current. No major shift is antenna characteristic was observed.

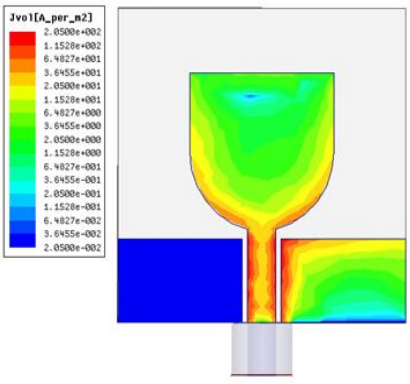

Fig9: Surface current distribution of Antenna 2

DOI: 10.46121/pspc.54.1.43

Power System Protection and Control
ISSN:1674-3415

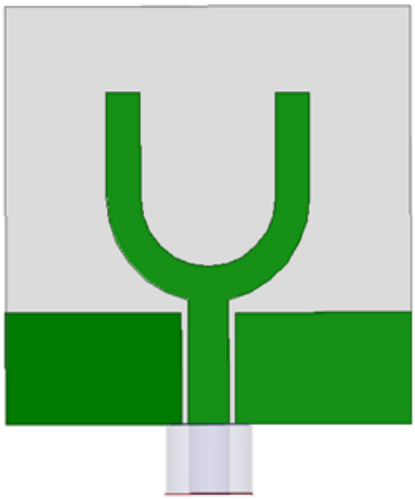

Fig10: Antenna 3: Antenna 2 with slot in the radiator

Antenna 3: A U-shaped slot was cut in the radiator since a weak current distribution strength was observed in the top and the center part of the radiator. Etching the U slot in the radiator also increases the current path and we observe two distinct resonance frequencies at 2.5 GHz and 4.3 GHz

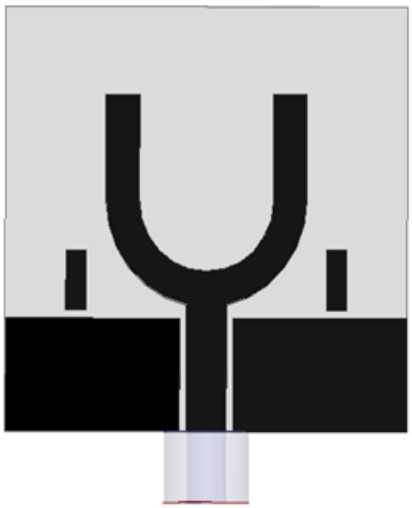

Fig11: Antenna 4: Antenna 3 with parasitic radiators

Antenna 4: Two short vertical strips, one on each side of the feed, near the inner edges of the U-arms, which are Electromagnetically coupled and not directly fed. These are λg/4 parasitic resonators tuned for 5.5 GHz, resulting in resonance at 2.5 GHz, 3.3 GHz, and 5.5 GHz and thus providing the triple-band operation. These parasitic elements alter the surface current distribution of the antenna, resulting in triple-band operation.

DOI: 10.46121/pspc.54.1.43

Power System Protection and Control
ISSN:1674-3415

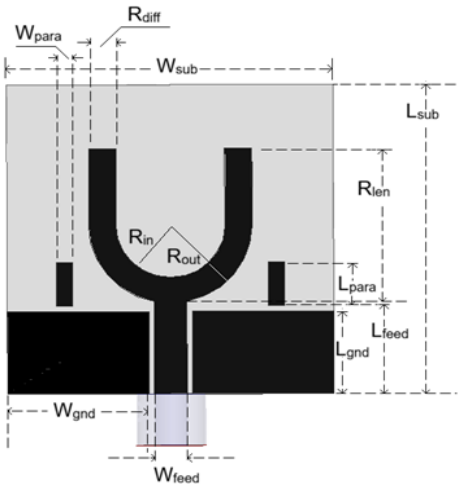

Fig12: Antenna 4 structure and dimensions

Parameter	Dimension (mm)	Parameter	Dimension (mm)
Rout	7.5 mm	Wgnd	13 mm
Rin	5 mm	Lgnd	8 mm
Rdiff	2.5 mm	Wsub	30 mm
Rlen	15 mm	Lsub	30 mm
Lfeed	8.95 mm	Wfeed	3 mm
Lpara	4.25 mm	Wpara	1.5 mm

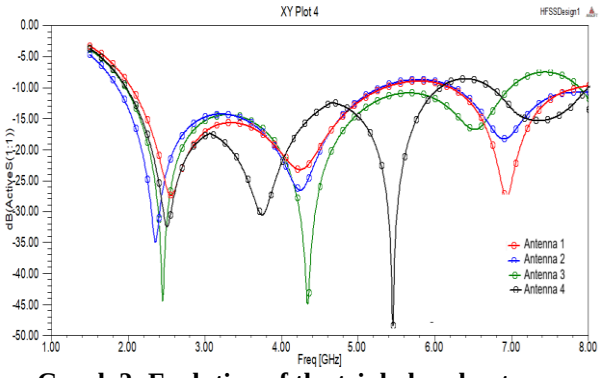

Graph 2: Evolution of the triple-band antenna

Operation of Parasitic element

Parasitic strips introduce an additional resonance through near-field coupling with the driven radiator. The strip length is designed as a quarter of the guided wavelength

$$L_p \approx \frac{\lambda_g}{4} = \frac{c}{4f\sqrt{\varepsilon_{\text{eff}}}}$$

DOI: 10.46121/pspc.54.1.43

Power System Protection and Control
ISSN:1674-3415

so that strong induced currents create a new resonant band with minimal impact on existing modes. For 5.5 GHz,

$$\lambda_0 = \frac{3 \times 10^8}{5.5 \times 10^9} = 54.5 \text{ mm}$$

$$\lambda_g = \frac{54.5}{\sqrt{2.7}} = 33.2 \text{ mm}$$

$$L_p = \frac{33.2}{4} = 8.3 \text{ mm}$$

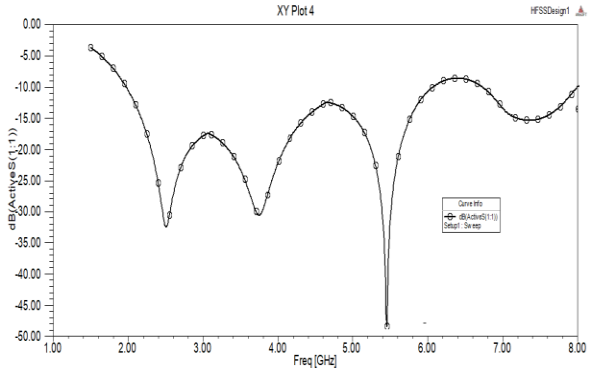

Graph3: Characteristics of the Triple-band antenna (S11)

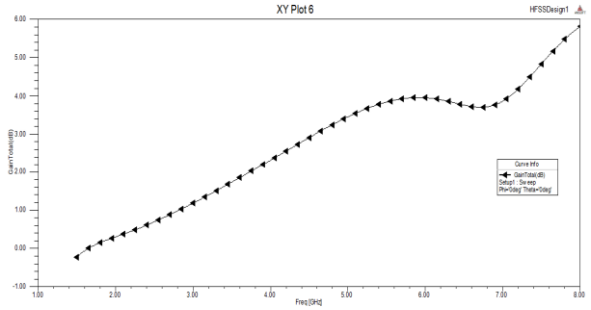

Graph4: Characteristics of the Triple-band antenna (Gain)

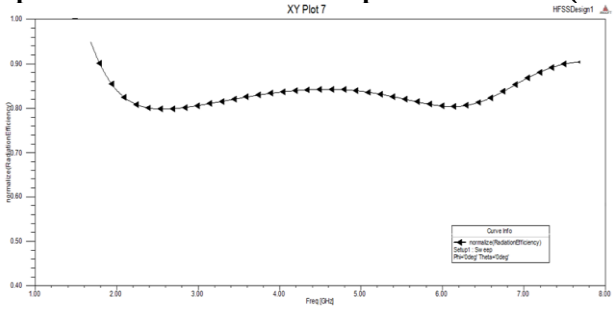

Graph5: Characteristics of the Triple-band antenna (Efficiency)

Characteristics of the Triple-band antenna (Radiation Pat.)

DOI: 10.46121/pspc.54.1.43

Power System Protection and Control
ISSN:1674-3415

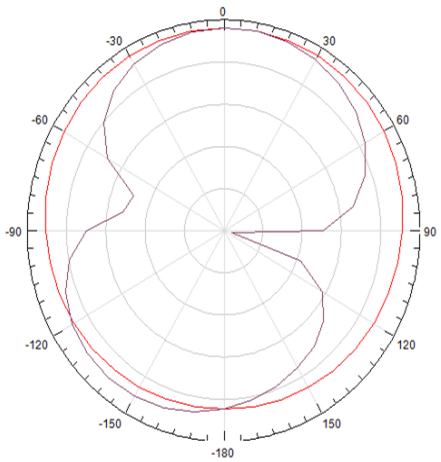

Fig12: Radiation patterns at 2.45 GHz

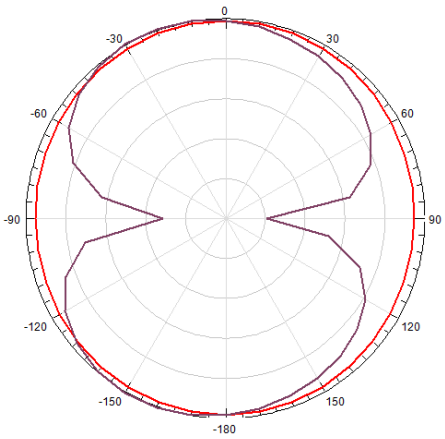

Fig13: Radiation patterns at 3.5 GHz

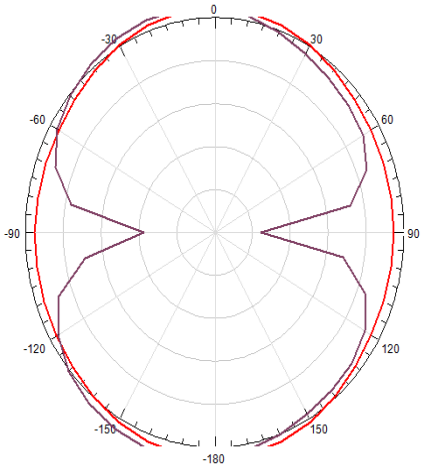

Fig14: Radiation patterns at 5.5 GHz

OBSERVATION

The appearance of a resonance at 6.5 GHz in a circular patch antenna designed for 2.45 GHz can potentially be attributed to harmonic resonance behavior. Although 6.5 GHz is not an exact integer multiple of 2.45 GHz, it is approximately 2.65 times higher, which suggests that it may be a nonlinear harmonic or spurious resonance

DOI: 10.46121/pspc.54.1.43

Power System Protection and Control
ISSN:1674-3415

introduced by the combined effects of the antenna's geometry, substrate characteristics, and feed structure. In particular, the use of a coplanar waveguide (CPW) feed can support a wider bandwidth and allow stronger coupling to higher-order or harmonic frequencies. The physical length of the feedline, as well as any discontinuities or transitions in the structure, can act as resonant elements themselves, introducing unintended resonances. Additionally, dielectric loading from the substrate can alter the effective wavelength in the structure, leading to slight deviations from ideal harmonic multiples. As a result, even though the design is optimized for 2.45 GHz, a higher-order or harmonic mode can manifest around 6.5 GHz, especially if not intentionally suppressed. This kind of behavior is common in compact micro strip or CPW-fed antennas, where higher-order and harmonic modes can be inadvertently excited.

PARAMETRIC STUDY

Effect of Feed Width (Fwidth) Variation on S11 Response

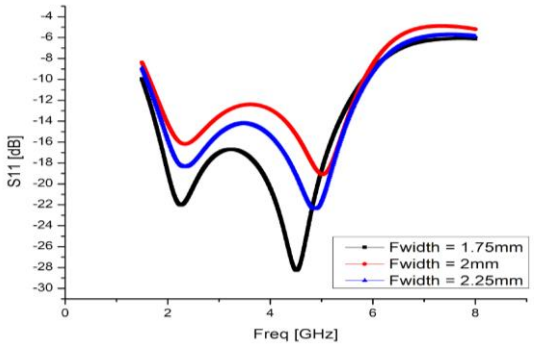

Graph6: Effect of Feed Width (Fwidth) Variation on S11 Response

Above Graph 2 Shows Decreasing the feed width improves impedance matching and enhances return loss characteristics at resonant frequencies. However, an optimal width must be selected considering fabrication tolerances and power handling

Effect of Radius (R) Variation on S11 Response

The graph 2 plot shown in below figure compares the performance of the antenna for three different radius values (R = 8.15 mm, 9.15 mm, and 10.15 mm). The variation in radius affects both the resonant frequencies and the return loss characteristics. The radius of the patch element (or a related circular dimension) significantly affects the antenna's resonant behavior. A moderate radius (9.15 mm in this case) offers optimal impedance matching and bandwidth, while too small or too large radii lead to detuning and reduced return loss.

Optimized Simulated Antenna Parameter Study

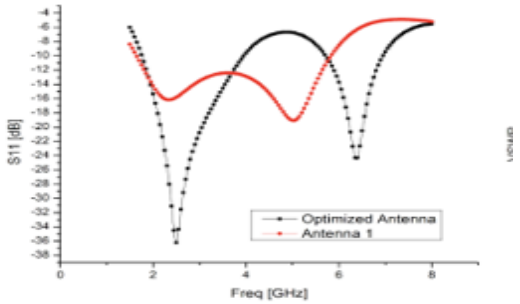

Graph7: Comparison of simulated S11

DOI: 10.46121/pspc.54.1.43

Power System Protection and Control
ISSN:1674-3415

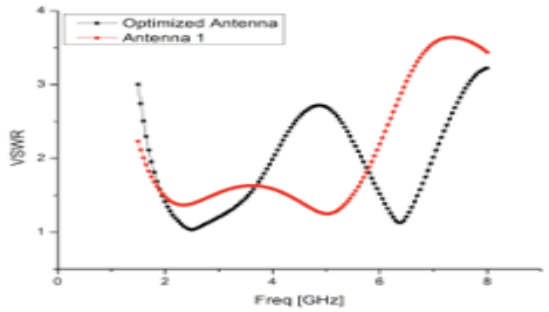

Graph8: Comparison of simulated VSWR

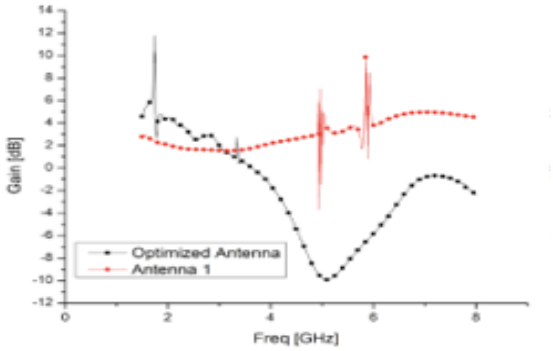

Graph9: Comparison of the simulated Gain

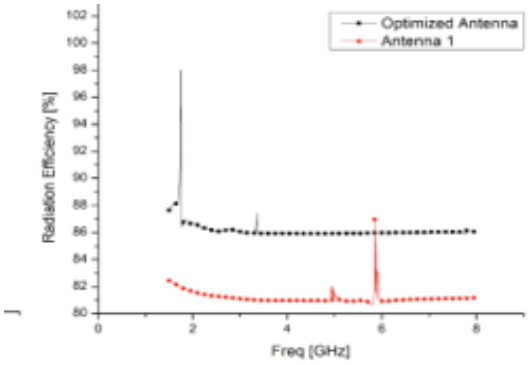

Graph10: Comparison of the Simulated Radiation Efficiency of Antenna 1 and Optimized Antenna

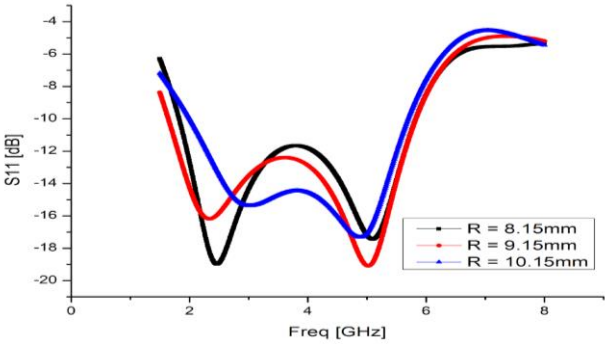

Graph11: Effect of Ground Length (Glen) Variation on S11 Response

The plot shown in below Fig. illustrates the S11 parameter for three different ground lengths: 12.5 mm, 13.5 mm, and 14.5 mm. The variation in Glen has a notable effect on the impedance matching and resonance characteristics of the antenna.

DOI: 10.46121/pspc.54.1.43

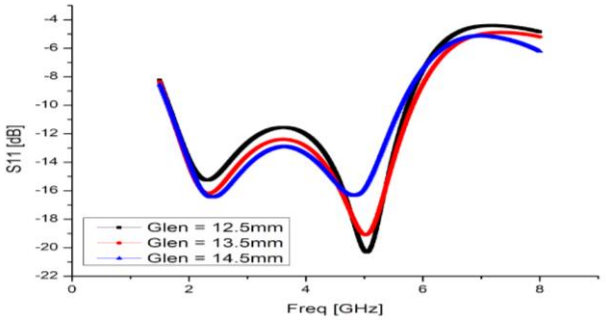

Graph 12: Effect of Ground Length (Glen) Variation on S11 Response

Parametric Study Result of 1×1 MIMO Antenna

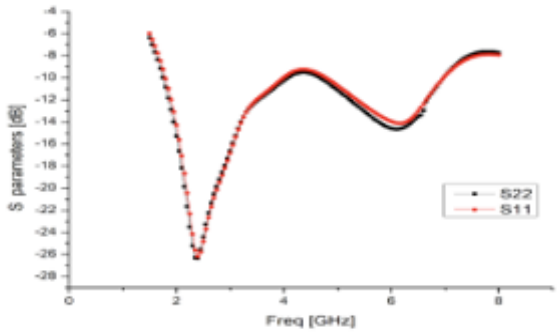

Graph13: Simulated S parameters

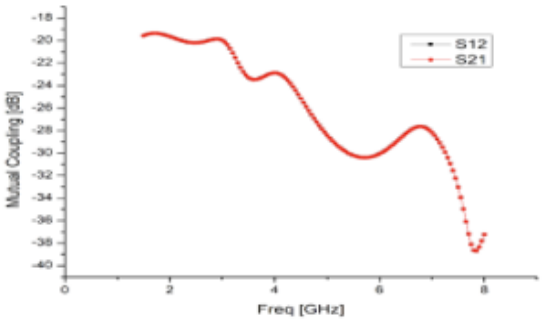

Graph 14: Mutual Coupling characteristics

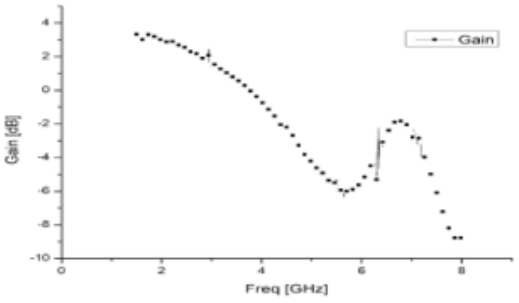

Graph 15: Simulated Gain

DOI: 10.46121/pspc.54.1.43

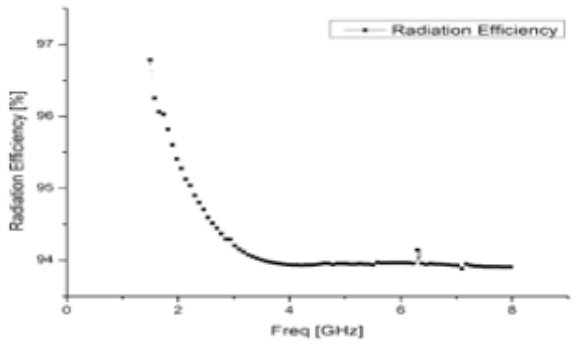

Graph 16: Simulated Radiation Efficiency

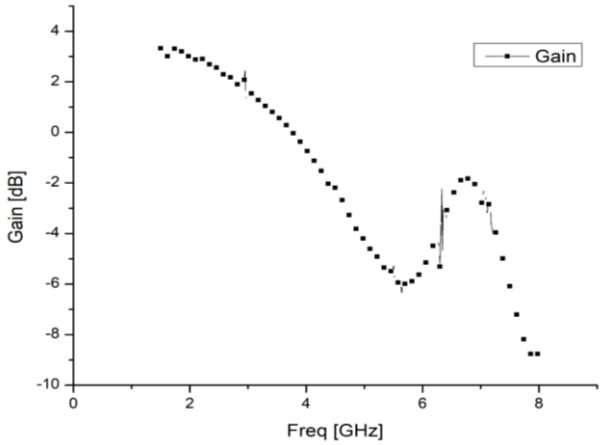

Graph17: Simulated Gain

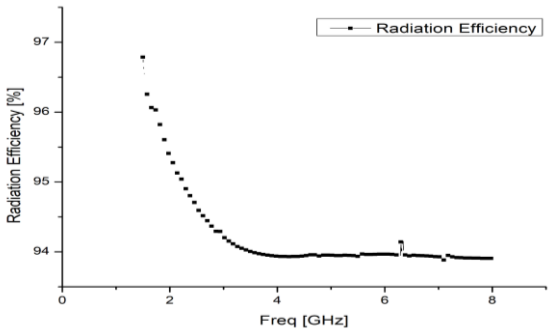

Graph 18: Simulated Radiation Efficiency

- Envelope Correlation Coefficient (ECC) and Diversity Gain (DG) are two important performance metrics used to evaluate the effectiveness of MIMO (Multiple Input Multiple Output) antenna systems.
- They indicate how well two or more antennas work together to improve signal quality and reliability, especially in fading environments

DOI: 10.46121/pspc.54.1.43

Power System Protection and Control
ISSN:1674-3415

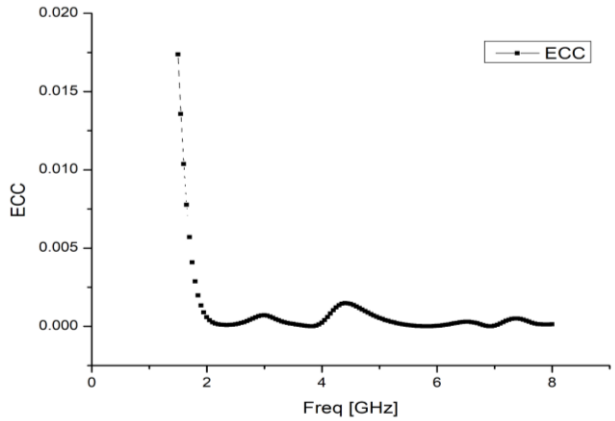

Graph 19: Simulated ECC of 1x1 MIMO antenna

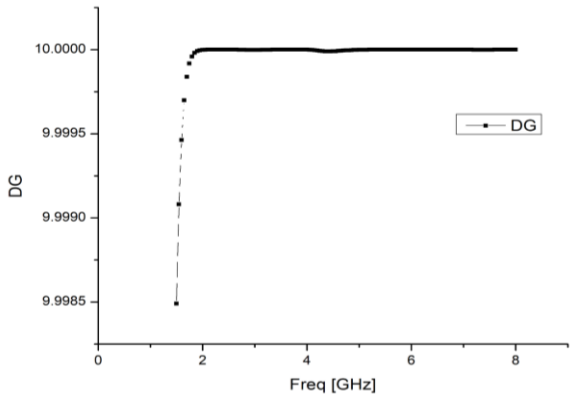

Graph 20: Simulated Diversity Gain

The mutual coupling characteristics of the proposed antenna configuration, highlighting the level of electromagnetic interaction between antenna elements across the operating frequency range. The observed low coupling values indicate effective isolation between ports, which is essential for achieving reliable MIMO performance and minimizing signal interference in compact antenna layouts. Graph 10 presents the simulated gain response of the antenna, demonstrating stable gain behavior across the targeted Sub-6 GHz frequency band, while Graph 11 shows the corresponding simulated radiation efficiency, confirming that the antenna maintains high efficiency with minimal power loss during radiation. In contrast, Graph 12 further illustrates the gain performance under an alternative operating condition or configuration, revealing consistent gain enhancement and validating the robustness of the antenna design, whereas Graph 13 depicts the simulated radiation efficiency for the same configuration, indicating sustained efficiency levels suitable for practical wireless applications.

Envelope Correlation Coefficient (ECC) and Diversity Gain (DG) are critical parameters used to evaluate the diversity performance of MIMO antenna systems, as they reflect how effectively multiple antenna elements operate together in multipath fading environments. Graph 14 shows the simulated ECC of the 1×1 MIMO antenna, where the low ECC values demonstrate minimal correlation between antenna ports, thereby ensuring improved diversity and enhanced signal reliability. Complementing this, Graph 15 illustrates the simulated diversity gain, which remains close to the ideal value, confirming that the antenna configuration provides strong diversity performance and effective mitigation of fading effects.

The current distribution and radiation characteristics further substantiate the antenna's operational effectiveness. Fig. 6 illustrates the simulated surface current distribution at 2.45 GHz for the 1×1 MIMO antenna configuration, revealing strong current concentration along the radiating edges and feed region, which confirms the excitation of the intended resonant mode. Meanwhile, Fig. 7 shows the simulated radiation characteristics at 2.45 GHz, demonstrating a stable and nearly omnidirectional radiation pattern suitable for Sub-6 GHz wireless communication. Collectively, these graphs and figures validate the antenna's capability to achieve low mutual

DOI: 10.46121/pspc.54.1.43

coupling, adequate gain, high radiation efficiency, and strong diversity performance, making it well suited for MIMO-based Sub-6 GHz applications.

Parametric Study: Rout

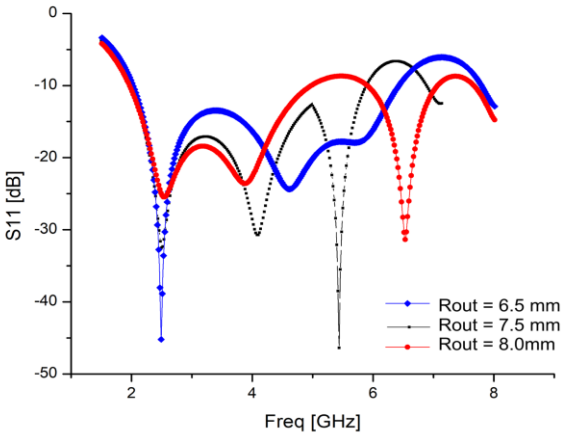

Graph 21: Effect of Ground Length (Rout) Variation on S11 Response

Observations: Variation in Rout significantly shifts the higher-order resonances by altering the effective current path length of the U-shaped radiator. A smaller Rout improves lower-band matching but disturbs mid/high-band stability, while a larger Rout shifts the upper resonance and weakens impedance matching. The optimized value Rout=7.5 mm provides the best overall multiband performance.

Parametric Study: Rin

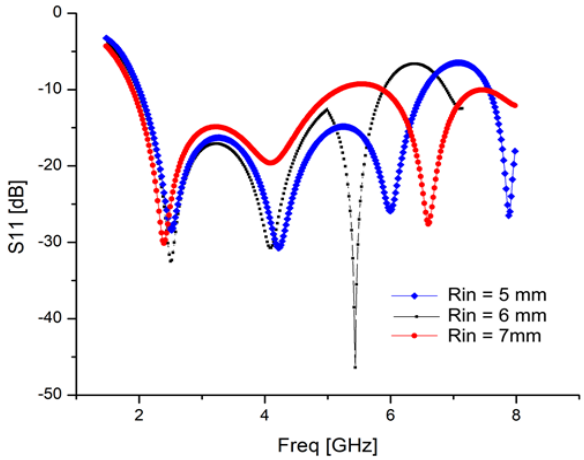

Graph 22: Effect of Ground Length (Rin) Variation on S11 Response

Observations: Variation in Rin mainly affects the coupling and tuning of the middle and upper resonant modes by modifying the current distribution inside the U-shaped radiator. A smaller Rin shifts resonances toward higher frequencies, while a larger Rin weakens matching and broadens the response. The optimized value Rin=5 mm provides stable multiband impedance matching.

Parametric Study: Lpara

DOI: 10.46121/pspc.54.1.43

Power System Protection and Control
ISSN:1674-3415

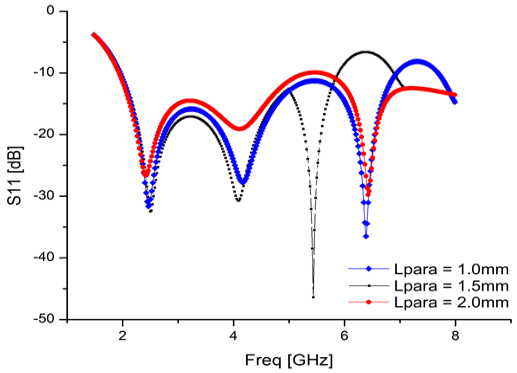

Graph 23: Effect of Ground Length (Lpara) Variation on S11 Response

Observations: The length of the parasitic vertical strips Lpara mainly controls the coupling strength between the strips and the main U-shaped radiator, significantly affecting the mid and upper resonant bands. Increasing Lpara shifts resonances slightly lower and smoothens impedance matching, while shorter lengths enhance higher-frequency response. The optimized Lpara=1.5 mm provides balanced multiband matching.

Parametric Study: Wpara

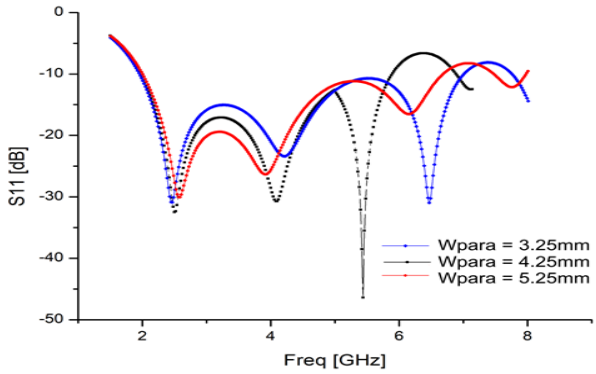

Graph 24: Effect of Ground Length (Wpara)Variation on S11 Response

Observations: The width of the parasitic vertical strips Wpara mainly influences the coupling capacitance between the strips and the main radiator, thereby affecting impedance matching and resonance strength. Increasing Wpara broadens the response but weakens higher-frequency matching, while a smaller width enhances sharper upper-band resonance. The optimized Wpara=4.25 mm achieves balanced multiband performance.

Parametric Study: Wsub

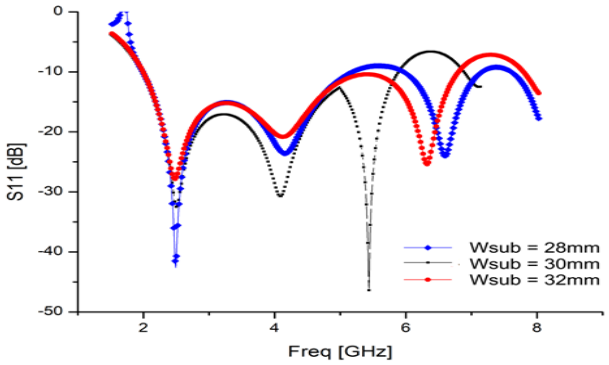

Graph 25: Effect of Ground Length (Wsub)Variation on S11 Response

Observations: The substrate width Wsub influences overall impedance matching by changing the effective ground coupling and fringing fields around the radiator. A smaller Wsub strengthens the lower-band resonance but disturbs

DOI: 10.46121/pspc.54.1.43

upper-band stability, while a larger Wsub broadens the response with slightly weaker matching. The optimized Wsub=30 mm achieves balanced multiband performance.

Parametric Study: Lsub

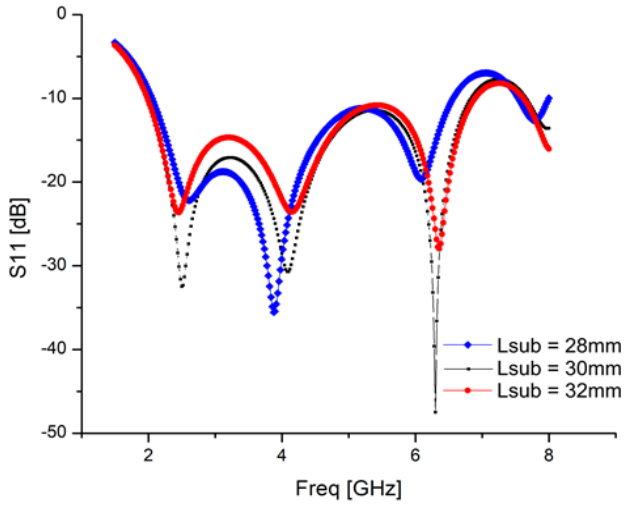

Graph 26: Effect of Ground Length (Wsub)Variation on S11 Response

Observations: The substrate length Lsub affects the effective electrical size and fringing fields, leading to shifts in resonance positions and impedance matching. A shorter Lsub enhances lower-band response, while a longer substrate improves upper-band tuning but slightly broadens the resonances. The optimized Lsub=30 mm provides stable multiband performance.

Parametric Study: Wgnd

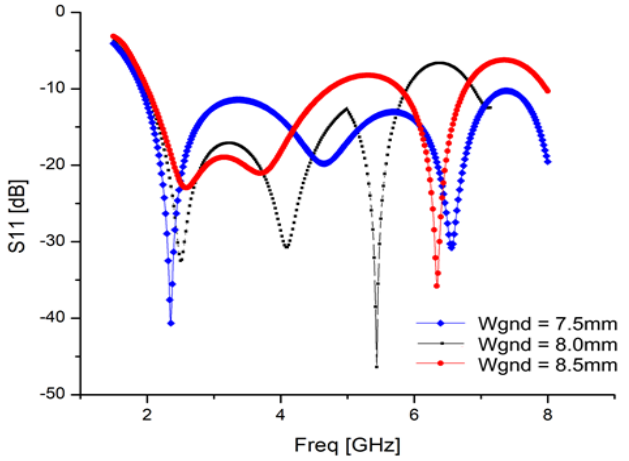

Graph 27: Effect of Ground Length (Wgnd)Variation on S11 Response

Observations: The ground width Wgnd strongly affects impedance matching by controlling the coupling between the feed line and radiating structure. A smaller Wgnd enhances lower-band resonance but degrades higher-frequency stability, while a larger Wgnd shifts resonances and weakens matching. The optimized Wgnd=8.0 mm provides balanced multiband performance.

Parametric Study: Lgnd

DOI: 10.46121/pspc.54.1.43

Power System Protection and Control
ISSN:1674-3415

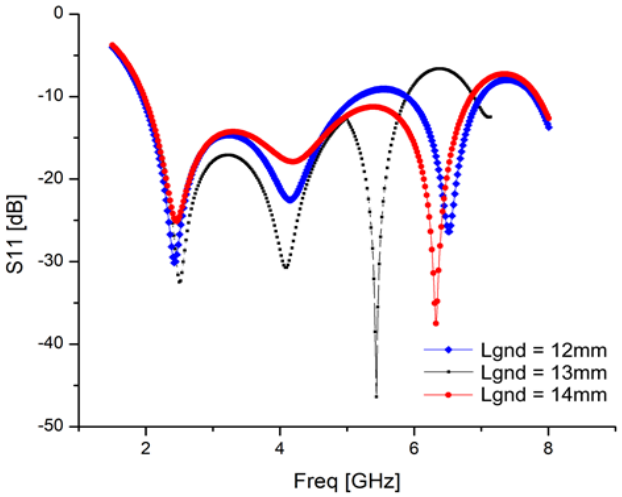

Graph 28: Effect of Ground Length (Lgnd)Variation on S11 Response

Observations: The ground length Lgnd significantly affects impedance matching and resonance tuning by modifying the current return path and coupling with the radiator. A shorter Lgnd enhances higher-frequency response, while a longer ground shifts resonances and slightly weakens matching. The optimized Lgnd=13 mm provides stable multiband performance.

Fabricated Prototype and measurement

DOI: 10.46121/pspc.54.1.43

Power System Protection and Control
ISSN:1674-3415

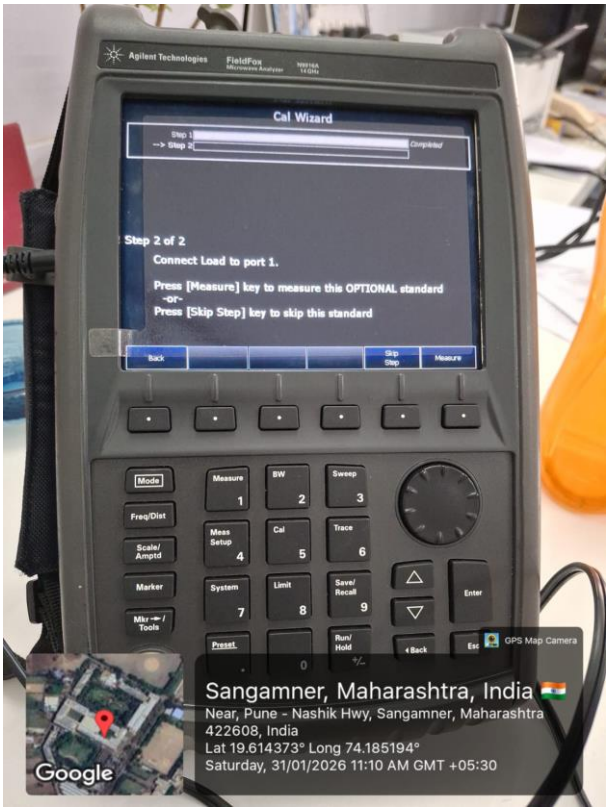

Measurement: The measurement is carried out using a 2 port Agilent 2N9916A 14 GHz VNA in an open-area network at Amrutvahini College of Engineering, Sangamner. The VNA is first calibrated before taking the measurements.

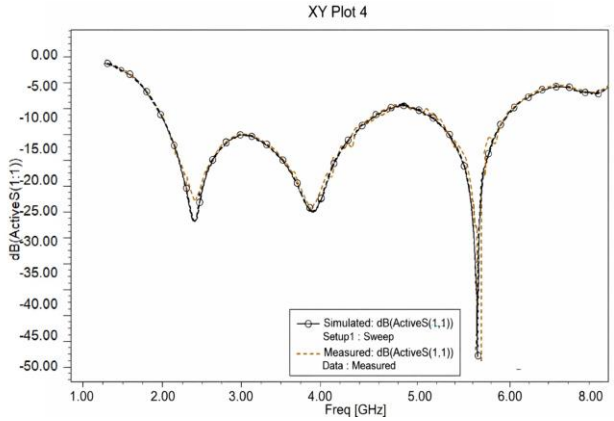

Graph 29: Simulated Vs Measured Return loss

CONCLUSION

In conclusion, this study successfully demonstrates the design, simulation, and performance evaluation of a Sub-6 GHz antenna configuration with a strong foundation for MIMO-based wireless communication systems. The mutual coupling analysis presented in Graph 9 confirms effective isolation between antenna elements, which is critical for minimizing inter-port interference and enhancing overall MIMO performance. The simulated gain and radiation efficiency characteristics shown in Graphs 10 to 13 indicate stable gain behavior and consistently high radiation efficiency across the operating frequency range, validating the suitability of the antenna for practical Sub-6 GHz applications. Furthermore, the diversity performance analysis highlights the effectiveness of the proposed configuration, where Graph 14 shows low Envelope Correlation Coefficient (ECC) values, signifying minimal correlation between antenna elements, and Graph 15 demonstrates a diversity gain close to the theoretical optimum,

DOI: 10.46121/pspc.54.1.43

ensuring reliable operation in multipath fading environments. The electromagnetic behavior of the antenna is further confirmed through field analysis, where Fig. 6 illustrates a well-distributed surface current at 2.45 GHz, indicating proper excitation of the resonant mode, and Fig. 7 shows stable and near-omnidirectional radiation characteristics suitable for wireless communication systems. Overall, the results collectively confirm that the proposed antenna structure achieves low mutual coupling, adequate gain, high radiation efficiency, and excellent diversity characteristics, establishing a strong platform for future extension toward compact tri-band MIMO antenna designs for advanced Sub-6 GHz and 5G wireless applications.

REFERENCES

1. Shobhit K. Patel et al., "Design and measurement of a compact MIMO antenna using C-shaped metamaterial for 5G/6G wireless communication circuit" Alexandria Engineering Journal, Elsevier, Volume 118, 2025, Pages 159-173. https://doi.org/10.1016/j.aej.2024.12.121
2. Chengzhu Du et al., "Design of tri-band flexible CPW 4-port slot MIMO antenna for conformal 5G, WIFI 6/6E and X-band applications" Engineering Science and Technology, an International Journal, Elsevier, Volume 62, 2025,Page No. 101937.
3. Ming-A Chung et al., "A Compact Multi-Band MIMO Antenna with High Isolation and Low SAR for LTE and Sub-6 GHz Applications" IEEE, 2025, Page No. 46014 – 46029. https://ieeexplore.ieee.org/document/10921639
4. Anouar Es-saleh et al., "Design aspects of MIMO antennas and its applications: A comprehensive review" Results in Engineering, Elsevier, Volume 25, 2025,Page No. 103797. https://doi.org/10.1016/j.rineng.2024.103797
5. Ashish Kumar et al., "Development of semi-circular corner cut MIMO antenna for 5G-advanced and 6G automotive wireless applications" Results in Engineering, Elsevier, Volume 25, 2025, Page No.103805.https://doi.org/10.1016/j.rineng.2024.103805
6. Noora Salim et al., "Comparative performance analysis of two novel design MIMO antennas for 5G and Wi-Fi 6 applications" Results in Engineering, Elsevier, Volume 25, 2025, Page No.103808. https://doi.org/10.1016/j.rineng.2024.103808
7. Manumula Srinubabu et al., "A compact and highly isolated integrated 8-port MIMO antenna for sub-6 GHz and mm-wave 5G-NR applications" Results in Engineering, Elsevier, Volume 25, 2025, Page No. 104068. https://doi.org/10.1016/j.rineng.2025.104068
8. Rakesh N. Tiwari et al., "Triple band lateral 4-port flexible MIMO antenna for millimeter wave applications at 24/28/38 GHz" Results in Engineering ,Elsevier, Volume 26, 2025, Page No.104678.https://doi.org/10.1016/j.rineng.2025.104678
9. Youssef Amraoui et al., "High isolation integrated four-port MIMO Antenna for terahertz communication" Results in Engineering, Elsevier, Volume 26,2025,Page No. 105253. https://doi.org/10.1016/j.rineng.2025.105253
10. Rania Hamdy Elabd et al., "Compact Circular MIMO Antenna with Defected Ground Structure (DGS) for Improved Isolation in 5G sub-6 GHz Mobile Systems" Results in
11. Ming-A Chung et al., "A 10 ×10Multi-Band MIMO Antenna System for LTE, 5G, Wi-Fi 7, and X-Band Communication Applications" IEEE Access, Volume 13, 2025.
12. Syed Misbah et al., "High Data-Rate Hilbert-Curved-Shaped MIMO Antenna with Improved

DOI: 10.46121/pspc.54.1.43

Bandwidth and Circular Polarization for Wireless Capsule Endoscopy" IEEE Access, Volume 13, 2025.

13. Fatih Özkan Alkurt, "Compact horn antenna design based on origami folding process for satellite communication" Advances in Space Research, Elsevier, Volume 75, Issue 11, 2025, Page No. 8280-8286. https://doi.org/10.1016/j.asr.2025.03.013
14. DAVID HERRAIZ et al., "High-Directivity and Low-Loss Directional Couplers Based on Empty Substrate Integrated Coaxial Line Technology" IEEE Access, Volume 12, 2024.
15. Widad Faraj A. Mshwat et al., "Compact Reconfigurable MIMO Antenna for 5G and Wi-Fi Applications" IEEE Access, Volume 12,2024.
16. Ayyaz Ali et al., "Design process of a compact Tri-Band MIMO antenna with wideband characteristics for sub-6 GHz, Ku-band, and Millimeter-Wave applications" Ain Shams Engineering Journal ,Elsevier, Volume 15, Issue 3, 2024,Page No. 102579. https://doi.org/10.1016/j.asej.2023.102579
17. V N Koteswara Rao Devana et al., "A high bandwidth dimension ratio compact super wide band-flower slotted microstrip patch antenna for millimeter wireless applications" Heliyon,Volume10, Issue1, 2024,Page No. e23712 https://doi.org/10.1016/j.heliyon.2023.e23712
18. Islem Bouchachi et al., "Design and performances improvement of an UWB antenna with DGS structure using a grey wolf optimization algorithm" Volume 10, Issue 5, 2024. Volume 10, Issue 5,Page No. e26337, 2024. https://doi.org/10.1016/j.heliyon.2024.e26337
19. Porchelvi Natarajan et al., "Design implementation analysis of multi-band antenna for terrestrial applications" Volume 10, Issue 18, 2024, Page No.e37519. https://doi.org/10.1016/j.heliyon.2024.e37519
20. Amraoui Youssef et al., "A new approach to designing a multiband antenna using photonic crystals and load graphene for terahertz application" Results in Engineering, Elsevier, Volume 22, 2024, Page No.102327. https://doi.org/10.1016/j.rineng.2024.102327
21. Youssef Amraoui et al., "High isolation MIMO antenna array for multiband terahertz applications" Results in Engineering, Elsevier, Volume 23, 2024,Page No. 102842 https://doi.org/10.1016/j.rineng.2024.102842
22. Md Afzalur Rahman et al., "Miniaturized tri-band integrated microwave and millimetre-wave MIMO antenna loaded with metamaterial for 5G IoT applications" Results in Engineering, Elsevier, Volume 24, 2024, Page No.103130 https://doi.org/10.1016/j.rineng.2024.103130
23. Vikash Kumar Jhunjhunwala et al., "A four port flexible UWB MIMO antenna with enhanced isolation for wearable applications" Results in Engineering, Elsevier, Volume 24, 2024, Page No.103147. https://doi.org/10.1016/j.rineng.2024.103147
24. Christina Josephine Malathi Andrews et al., "Compact Metamaterial based Antenna for 5G Applications" Results in Engineering, Elsevier, Volume 24, 2024, Page No.103269. https://doi.org/10.1016/j.rineng.2024.103269
25. Md. Sohel Rana et al., "Machine learning based on patch antenna design and optimization for

DOI: 10.46121/pspc.54.1.43

5 G applications at 28GHz" Results in Engineering, Elsevier, Volume 24, 2024, Page No. 103366. https://doi.org/10.1016/j.rineng.2024.103366

26. Xi Wang Dai et al., "High isolation MIMO antenna designed with tightly coupled microstrip patch pairs" AEU - International Journal of Electronics and Communications, Elsevier, Volume 177, 2024, 155169. https://doi.org/10.1016/j.aeue.2024.155169
27. Md. Ziaul Islam et al., "Development of a Smart Antenna for Wireless Communication in ISM Band" IEEE, 2024. https://ieeexplore.ieee.org/document/10491065
28. Tapan Nahar et al., "Leaf-Shaped Antennas for Sub-6 GHz 5G Applications" IEEE, 2024, Page No. 114338 – 114357. https://ieeexplore.ieee.org/document/10614171
29. Yan-Ting Liu et al., "On the Directivity, Gain and Realized Gain of Polarization Reconfigurable Antenna" IEEE, 2024. https://ieeexplore.ieee.org/document/10699968
30. Musa Hussain et al., "Self-decoupled tri band MIMO antenna operating over ISM, WLAN and C-band for 5G applications" Heliyon, Volume 9, Issue 7, 2023,Page No.e17404.
31. Wahaj Abbas Awan et al., "Enhancing isolation performance of tilted Beam MIMO antenna for short-range millimeter wave applications" Heliyon, Volume 9, Issue 9, 2023, Page No. e19985.
32. Oluwatayomi Rereloluwa Adegboye et al., "Antenna S-parameter optimization based on golden sine mechanism based honey badger algorithm with tent chaos" Volume 9, Issue 11, 2023,Page No. e21596. https://doi.org/10.1016/j.heliyon.2023.e21596
33. Deepa Bammidi et al., "Design and validation of frequency reconfigurable multiband antenna using varied current distribution method" Measurement: Sensors, Elsevier, Volume 29, 2023, Page No.100844. https://doi.org/10.1016/j.measen.2023.100844
34. Azimov Uktam Fakhriddinovich et al., "A Compact Antenna with Multiple Stubs for ISM, 5G Sub-6-GHz, and WLAN" IEEE Access, Volume 11, 2023.
35. Hung Nguyen-Manh et al., "A Design of MIMO Antenna with High Isolation and Compact Size Characteristics" IEEE Access, Volume 11, 2023.
36. Seyed Saeid Mosavinejad et al., "A triple-band spiral-shaped antenna for high data rate fully passive implantable devices" AEU - International Journal of Electronics and Communications, Elsevier, Volume 159, 2023, Page No.154474. https://doi.org/10.1016/j.aeue.2022.154474
37. Parveez Shariff B. G. et al., "High-Isolation Wide-Band Four-Element MIMO Antenna Covering Ka-Band for 5G Wireless Applications" IEEE, 2023, Page No: 123030 – 123046. https://ieeexplore.ieee.org/document/10301425
38. Haiyang Miao et al., "Sub-6 GHz to mm Wave for 5G-Advanced and Beyond: Channel Measurements, Characteristics and Impact on System Performance" IEEE, 2023. https://ieeexplore.ieee.org/document/10121509
39. Haroon Ahmed et al., "Sub-6 GHz MIMO antenna design for 5G smartphones: A deep learning approach" AEU - International Journal of Electronics and Communications, Elsevier, Volume 168, 2023, Page No.154716. https://www.sciencedirect.com/science/article/abs/pii/S1434841123001905

DOI: 10.46121/pspc.54.1.43

40. S. J. Maeng et al., “Spectrum Activity Monitoring and Analysis for Sub-6 GHz Bands Using a Helikite” IEEE, 2023. https://ieeexplore.ieee.org/document/10041314
41. D. Allin Joe et al., “2 X 2 MIMO Antenna Design For 5G Applications” IEEE, 2023. https://ieeexplore.ieee.org/document/10199993
42. Suverna Sengar et al., “A Compact Tri-band Microstrip Patch Antenna Design for 5G millimeter wave applications” IEEE, 2023. https://ieeexplore.ieee.org/document/10308282
43. Gouree Shankar Das et al., “Compact four elements SUB-6 GHz MIMO antenna for 5G applications” Elsevier, 2023. https://doi.org/10.1016/j.matpr.2023.06.344
44. Liton Chandra Paul et al., “A slotted plus-shaped antenna with a DGS for 5G Sub-6 GHz/WiMAX applications” Heliyon, Volume 8, Issue 12, 2022,Page No.e12040.
45. M. Kamran Shereen et al., “A review of achieving frequency reconfiguration through switching in microstrip patch antennas for future 5G applications” Alexandria Engineering Journal, Elsevier, Volume 61, Issue 1, 2022, Pages 29-40. https://doi.org/10.1016/j.aej.2021.04.105
46. Geng Zhang et al., “Design of a new anti-metal RFID temperature tag antenna based on short-circuit stub structure” Procedia Computer Science, Elsevier, 2022, Page No.367–374. https://creativecommons.org/licenses/by-nc-nd/4.0)
47. R. Nagendra et al., “Design and performance of four port MIMO antenna for IOT applications” ICT Express, Elsevier, Volume 8, Issue 2, 2022, Pages 235-238. https://doi.org/10.1016/j.icte.2021.05.008
48. Muhammad Noaman Zahid et al., “H-Shaped Eight-Element Dual-Band MIMO Antenna for Sub-6 GHz 5G Smartphone Applications” IEEE Access, Volume 10, 2022.
49. Abdullah J. Alazemi et al., “A High Data Rate Implantable MIMO Antenna for Deep Implanted Biomedical Devices” IEEE Transactions on Antennas and Propagation, Volume: 70, Issue: 2, 2022.
50. Amin Al Ka'bi et al., “Proposed Antenna Design for IoT and 5G-WiFi Applications” IEEE,2022. https://doi.org/10.1109/AIIoT54504.2022.9817261
51. Anita Rani et al., “A Compact MIMO Antenna with High Isolation and Gain-Bandwidth Product for Wireless Personal Communication” IEEE, 2022. https://ieeexplore.ieee.org/document/9787672
52. Amol D Sonawane et al., “Half Wave Dipole Antenna Performance Parameter Measurement and Comparison at 900 and 1800 MHz Frequency” IEEE, 2022. https://ieeexplore.ieee.org/document/9952418
53. Yuwei Zhang et al., “Simulation Design of Pattern Reconfigurable Antenna Based on Liquid Metal Switch” IEEE, 2022. https://ieeexplore.ieee.org/document/9886113
54. P Prakash et al., “MIMO Antenna System for IoT Applications (5G)” IEEE, 2022. https://ieeexplore.ieee.org/document/9780845
55. Aamna Ali Alblooshi et al., “Design of 2×2 MIMO Antenna for Sub-5G IoT Applications” IEEE,

DOI: 10.46121/pspc.54.1.43

2022. https://ieeexplore.ieee.org/document/9791812

56. Kamel Sultan et al., "A Multiband Multibeam Antenna for Sub-6 GHz and mm-Wave 5G Applications" IEEE, 2022, Page. 1278 – 1282. https://ieeexplore.ieee.org/document/9748985
57. Amany A. Megahed et al., "Sub-6 GHz Highly Isolated Wideband MIMO Antenna Arrays" 2022, Page No.19875 – 19889 https://ieeexplore.ieee.org/document/9709315
58. S. Kannadhasan et al., "Performance, Metrics, and Challenges of Multiband Antenna for Wireless Communication" IEEE, 2022. https://ieeexplore.ieee.org/document/9776735
59. Md. Sohel Rana et al., "Study of Microstrip Patch Antenna for Wireless Communication System" IEEE, 2022. https://ieeexplore.ieee.org/document/9726110
60. ChienHsiang Wu et al., "A survey on improving the wireless communication with adaptive antenna selection by intelligent method" Computer Communications, Elsevier, Volume 181, 2022, Page No. 374-403. https://doi.org/10.1016/j.comcom.2021.10.034
61. Jyoti Yadav et al., "A paper on microstrip patch antenna for 5G applications" Elsevier, Volume 66, Part 8, 2022, Page No. 3430-3437. https://doi.org/10.1016/j.matpr.2022.06.123
62. Poonam Kumari et al., "A Circularly Polarized Sub-6 GHz MIMO Antenna for 5G Applications" IEEE, 2022. https://ieeexplore.ieee.org/document/9886923
63. Hassan Tariq Chattha ET AL., "Compact Multiport MIMO Antenna System for 5G IoT and Cellular Handheld Applications" IEEE Xplore 2021.
64. Jungwoo Seo et al., "Miniaturized Dual-band Broadside/End fire Antenna-in-Package for 5G Smartphone" IEEE Xplore, 2021.
65. Md. Muzammil Sani et al., "Design and analysis of multiple input multiple output antenna for wideband applications using cylindrical dielectric resonator" International Journal of Electronics and Communications, Elsevier ,Volume 131, 2021,page no. 153598, https://doi.org/10.1016/j.aeue.2020.153598
66. Uzair Ahmad et al., "MIMO Antenna System with Pattern Diversity for Sub-6 GHz Mobile Phone Applications" IEEE Access, Volume 9, 2021.
67. Guizhi Xu et al., "Design of non-dimensional parameters in stretchable microstrip antennas with coupled mechanics-electromagnetics" Materials & Design, Elsevier, Volume 205, 2021,Page No. 109721. https://doi.org/10.1016/j.matdes.2021.109721
68. Devesh Kumar et al., "Frequency reconfigurable Microstrip Patch Antenna with an Arc-shaped cut" IEEE Xplore,2021.
69. Jing Luo et al., "Design of Compact Tri-Band MIMO Antenna Using Decoupling Structures for 5G Mobile Terminals" IEEE, 2021. https://ieeexplore.ieee.org/document/9631685
70. Ho Jung Nam et al., "Tunable Triple-Band Antenna for Sub-6 GHz 5G Mobile Phone" IEEE, 2021. https://ieeexplore.ieee.org/document/9330484

DOI: 10.46121/pspc.54.1.43

71. Rifaqat Hussain et al., “5G MIMO Antenna Designs for Base Station and User Equipment: Some recent developments and trends” IEEE, 2021, Page No.95 – 107. https://ieeexplore.ieee.org/document/9478857
72. Shivani Chandra et al., “Design and Simulation of Graphene Based Antenna for Radiation Pattern” IEEE, 2021. https://ieeexplore.ieee.org/document/9417938
73. Saeed I. Latif et al., “Frequency Reconfigurable Antennas” IEEE, 2021, Page No.19 – 66. https://ieeexplore.ieee.org/document/9432037
74. Shivleela Mudda et al., “Compact High Gain Microstrip Patch Multi-Band Antenna for Future Generation Portable Devices Communication” IEEE, 2021. https://ieeexplore.ieee.org/document/9396776
75. Naser Ojaroudi Parchin et al., “A New Broadband MIMO Antenna System for Sub 6 GHz 5G Cellular Communications” IEEE, 2020. https://ieeexplore.ieee.org/document/9135546
76. Wang Yibo et al., “ Bandwidth enhanced miniaturized slot antenna on a thin microwave laminate” International Journal of Electronics and Communications, Elsevier Volume127, 2020,page no.153475. https://doi.org/10.1016/j.aeue.2020.153475
77. Balaka Biswas ET AL., “Fractal inspired miniaturized wideband ingestible antenna for wireless capsule endoscopy” International Journal of Electronics and Communications (AEÜ), Elsevier Volume 120, 2020,PAPRE NO. 153192 https://doi.org/10.1016/j.aeue.2020.153192
78. Mohammad Muzammil Sani et al., “An Ultra-Wideband Rectangular Dielectric Resonator Antenna with MIMO Configuration” IEEE Access, Volume 8, 2020.
79. Wa’il A. Godaymi Al-Tumah et al., “Design, simulation and measurement of triple band annular ring microstrip antenna based on shape of crescent moon” International Journal of Electronics and Communications (AEÜ), Volume 117, 2020, page no. 153133. https://doi.org/10.1016/j.aeue.2020.153133
80. Shrenik Suresh Sarade et al., “Development of Multiband MIMO Antenna with Defective Ground Structure: Review” Procedia Computer Science, Elsevier,2020. http://creativecommons.org/licenses/by-nc-nd/4.0/

DOI: 10.46121/pspc.54.1.43